Enhanced Mechanical Fault Diagnosis of High-Voltage Circuit Breakers Using a Multi-Strategy Improved Dung Beetle Algorithm and Support Vector Machine

Min Lu *, Sifan Yuan , Anan Zhou , Jiawei Guo , Jie Yu , Guangtao Zou , Aimin Zhang , Jing Yan

Posted Date: 28 January 2026

doi: 10.20944/preprints202601.2178.v1

Keywords: high-voltage circuit breaker; fault diagnosis; multi-strategy improved dung beetle optimization algorithm; support vector machine

Article

Enhanced Mechanical Fault Diagnosis of High-Voltage Circuit Breakers Using a Multi-Strategy Improved Dung Beetle Algorithm and Support Vector Machine

Min Lu [1,*], Sifan Yuan [2], Anan Zhou [3], Jiawei Guo [1], Jie Yu [1], Guangtao Zou [1], Aimin Zhang [4] and Jing Yan [3]

[1] Jiujiang Power Supply Branch, State Grid Jiangxi Electric Power Co., Ltd., Jiujiang 332000, China
[2] Electric Power Research Institute, State Grid Jiangxi Electric Power Co., Ltd., Nanchang 330006, China
[3] Xi'an Jiaotong University, Xi'an 710049, China
[4] Jiangxi Gandian Electric Co., Ltd., Fuzhou 344200, China
* Correspondence: jenifer.020324@gmail.com

Abstract

High-voltage circuit breakers (HVCBs) are critical switching devices whose mechanical reliability directly affects the safe and stable operation of power systems. However, accurate fault diagnosis of HVCBs remains challenging due to complex mechanical structures, nonlinear vibration characteristics, and sensitivity to parameter selection in data-driven models. To address these issues, this paper proposes an enhanced mechanical fault diagnosis method based on a multi-strategy improved dung beetle optimization–support vector machine (MIDBO-SVM) framework. First, mechanical vibration signals under four typical operating conditions of HVCBs are collected, and discriminative frequency-domain features are extracted using the fast Fourier transform. To overcome the limitations of conventional SVMs in parameter tuning, a multi-strategy improved dung beetle optimization (MIDBO) algorithm is developed by integrating adaptive search mechanisms to enhance global exploration and convergence efficiency. The proposed MIDBO is then employed to optimize the penalty and kernel parameters of the SVM, yielding a robust and well-generalized fault diagnosis model. Experimental results demonstrate that the MIDBO-SVM model exhibits superior convergence behavior and a stronger ability to escape local optima compared with standard optimization strategies. The proposed method achieves the highest diagnostic accuracy of 96.67% across multiple fault categories. Moreover, under imbalanced sample conditions, the MIDBO-SVM maintains high diagnostic accuracy and stability, effectively distinguishing different operating states of HVCBs. These results confirm the effectiveness and robustness of the proposed approach for mechanical fault diagnosis of HVCBs.

Keywords: high-voltage circuit breaker; fault diagnosis; multi-strategy improved dung beetle optimization algorithm; support vector machine

1. Introduction

As a critical protective and control device in power systems, the reliable operation of high-voltage circuit breakers (HVCBs) is essential to ensuring the safety and stability of the power grid. During long-term service, however, the operating mechanism and control circuit of HVCBs are among the components most susceptible to failure [1–3]. Factors such as spring fatigue, iron core jamming, and coil degradation during opening and closing operations may cause malfunction of the circuit breaker, potentially leading to severe power system disturbances or even cascading failures. Mechanical vibration signals generated during the operation of HVCBs contain abundant condition-

 doi:10.20944/preprints202601.2178.v1

related information, including action timing, amplitude, and frequency characteristics, which can effectively reflect the health status of mechanical components. In particular, vibration signals with a high signal-to-noise ratio provide valuable insight into the mechanical behavior of circuit breakers [4]. Consequently, timely and accurate monitoring and diagnosis of mechanical faults using vibration signal analysis have become indispensable for ensuring the safe and reliable operation of modern power systems [5–7].

With the rapid development of artificial intelligence technologies, fault diagnosis methods have gradually evolved toward intelligent and data-driven paradigms. Machine learning techniques, such as artificial neural networks and support vector machines (SVMs), have been widely applied to HVCB fault identification tasks [8,9]. Neural networks exhibit strong nonlinear mapping and self-learning capabilities, enabling them to extract complex fault features from data [10]. However, their practical application is often hindered by several limitations, including slow convergence, susceptibility to local optima, dependence on large training datasets, and the lack of a unified theoretical framework for network structure design, overfitting, and underfitting control. In contrast, SVMs construct an optimal separating hyperplane based on a limited number of support vectors and demonstrate strong generalization performance, particularly in small-sample, nonlinear, and high-dimensional classification problems [11]. Nevertheless, the classification performance of an SVM is highly sensitive to its hyperparameters, especially the penalty factor g and kernel parameter C. Improper parameter selection may not only degrade classification accuracy but also lead to prolonged training time and suboptimal convergence behavior [12,13]. Therefore, effective hyperparameter optimization is crucial for improving SVM-based fault diagnosis performance.

To address this issue, various intelligent optimization algorithms have been introduced to optimize SVM parameters in fault diagnosis applications. Zhao et al. [14] proposed a fault diagnosis method for circuit breaker energy storage systems by combining vibration-current features with a gray wolf optimization (GWO)–SVM framework, thereby mitigating the adverse effects of arbitrary parameter selection. Li et al. [15] employed wavelet packet decomposition for feature extraction and optimized SVM parameters using particle swarm optimization (PSO) to diagnose HVCB faults. Bie et al. [16] developed a bearing fault diagnosis approach based on adaptive noise-assisted empirical mode decomposition and PSO-SVM, achieving favorable pattern recognition performance. Yang et al. [17] introduced a mechanical fault diagnosis method for circuit breakers using principal component analysis and SVM, with the whale optimization algorithm applied for parameter tuning, resulting in improved classification accuracy. Yang et al. [18] compared SVM and backpropagation neural networks for dissolved oxygen fault diagnosis and utilized a genetic algorithm to enhance classification performance. Although swarm intelligence optimization algorithms have demonstrated effectiveness in global search and are relatively easy to implement, they still suffer from inherent drawbacks, such as premature convergence, insufficient population diversity, and an imbalance between global exploration and local exploitation. Consequently, their optimization accuracy and convergence robustness require further improvement, especially in complex engineering applications.

The dung beetle optimization (DBO) algorithm, proposed by Jiankai Xue and Bo Shen, is a novel metaheuristic inspired by the natural behaviors of dung beetles and characterized by five distinct position update strategies [19]. Owing to its fast convergence speed and strong global optimization capability, DBO has shown promising performance in various engineering problems. Li et al. [20] applied DBO to active disturbance rejection control and demonstrated its superiority over conventional ADRC and PID controllers. Zhang et al. [21] proposed a DBO-optimized neural network for short-term load forecasting, effectively addressing prediction challenges caused by random load fluctuations. Nevertheless, as no single swarm intelligence algorithm can guarantee optimal performance across all optimization scenarios, DBO also exhibits limitations, particularly in maintaining population diversity during iterative optimization. To overcome these shortcomings, several improved DBO variants have been proposed. Li et al. [22] incorporated a random differential variation strategy into DBO to reduce the risk of premature convergence, thereby enhancing the

 doi:10.20944/preprints202601.2178.v1

prediction accuracy and stability of a BiLSTM-based wind speed forecasting model. Li et al. [23] applied an improved DBO algorithm with reverse learning and fitness–distance balance strategies to robot path planning, achieving faster convergence and improved global search capability.

Motivated by the strong self-search ability and fast convergence characteristics of DBO, this study proposes a multi-strategy adaptive dung beetle optimization algorithm to further enhance global exploration and local exploitation balance for mechanical fault diagnosis of HVCBs. Specifically, an optimal point set strategy combined with circle chaotic mapping is employed to initialize the population, improving population diversity and ergodicity. Subsequently, a sine–cosine search strategy and adaptive weight factor are incorporated into the rolling dung beetle position update mechanism to guide the search process toward the global optimum with oscillatory decay behavior. Finally, a Cauchy–Gaussian mutation strategy is introduced to perturb the current best individual, expanding the search space and preventing premature convergence. The proposed improved DBO algorithm is integrated with an SVM classifier to construct a robust mechanical fault diagnosis framework for HVCBs. Extensive comparative experiments with other optimization algorithms are conducted to validate the effectiveness and practical engineering applicability of the proposed method.

2. Preliminaries

2.1. Support Vector Machine

Support vector machines (SVMs) are supervised learning models grounded in statistical learning theory and structural risk minimization. By introducing kernel functions, SVMs implicitly map input samples from a low-dimensional input space into a high-dimensional feature space, where complex nonlinear classification problems can be transformed into linearly separable ones [24,25]. Different kernel functions induce distinct feature space geometries, resulting in different data distributions and classification performance.

Consider a training dataset consisting of N labeled samples $\{(x_i, y_i)\}_{i=1}^{N}$, where $x_i \in \mathbb{R}^d$ denotes the input feature vector of the i-th sample and $y_i \in \{-1, +1\}$ represents the corresponding class label. In general, infinitely many hyperplanes can separate two linearly separable classes in the feature space [26]. The fundamental objective of SVM is to identify the optimal separating hyperplane that maximizes the margin between the two classes, thereby enhancing generalization performance.

The maximum-margin optimization problem can be formulated as:

$$\arg\max_{\boldsymbol{w},b}\left\{\min_{i}\left(y_i\bullet\left(\omega_i x_i+b\right)\right)\bullet\frac{1}{\|\boldsymbol{w}\|}\right\}, \tag{1}$$

where $\boldsymbol{\omega}$ denotes the weight vector and b is the bias term defining the decision boundary. The optimal hyperplane is determined exclusively by a subset of training samples, known as support vectors, which lie on or near the margin boundaries.

In practical applications, training data are often not strictly linearly separable. To accommodate this, SVM introduces the concept of a soft margin by incorporating slack variables $\xi_i \geq 0$, allowing a controlled degree of misclassification. The corresponding optimization problem based on the hinge loss function is expressed as:

$$\begin{cases}\arg\min\limits_{w,b,\xi}\dfrac{1}{2}\|\boldsymbol{w}\|^2+C\sum\limits_{i=1}^{n}\xi_i \\ s.t.\begin{cases}y_i\left(\boldsymbol{w}\cdot x_i+b\right)\geq 1, i=1,2,\cdots,n' \\ C\geq 0\end{cases}\end{cases} \tag{2}$$

 doi:10.20944/preprints202601.2178.v1

where $C > 0$ is the penalty parameter that balances margin maximization and empirical risk. A larger value of Cimposes a higher penalty on misclassified samples, resulting in a more complex decision boundary.

By applying the Lagrange multiplier method to the convex quadratic programming problem with inequality constraints and exploiting Lagrangian duality, the primal optimization problem can be transformed into its dual form. According to the Karush–Kuhn–Tucker (KKT) conditions [27], the dual objective function is given by:

$$\begin{cases} \max\limits_{\alpha} \sum\limits_{i=1}^{n} \alpha_i - \frac{1}{2} \sum\limits_{\substack{i=1 \\ j=1}}^{n} \alpha_i \alpha_j y_i y_j K(x_i, x_j) \\ \text{s.t.} \begin{cases} \sum\limits_{i=1}^{n} \alpha_i y_i = 0 \\ 0 \le \alpha_i \le C, i = 1, 2, \cdots, n \end{cases} \end{cases}, \tag{3}$$

where $\alpha_i$denotes the Lagrange multiplier associated with the i-th training sample, and $K(\cdot,\cdot)$ is the kernel function.

To address nonlinear classification problems, the radial basis function (RBF) kernel is commonly employed due to its strong nonlinear mapping capability and limited number of hyperparameters. The RBF kernel is defined as:

$$k(x, z) = \exp\left(-\frac{\|x - z\|^2}{2g^2}\right), \tag{4}$$

where g is the kernel parameter that controls the width of the Gaussian function. Through kernel mapping, samples that are nonlinearly separable in the original input space may become linearly separable in the induced high-dimensional feature space, as illustrated in Figure 1.

The final SVM decision function is therefore expressed as:

$$f(x) = sign\left(\sum_{\substack{i=1 \\ j=1}}^{n} \alpha_i y_i K(x_i, x_j) + b\right), \tag{5}$$

where the classification performance is jointly determined by the penalty parameter C and the kernel parameter g. Consequently, appropriate selection and optimization of these hyperparameters are critical for achieving optimal classification accuracy and generalization capability in SVM-based fault diagnosis tasks.

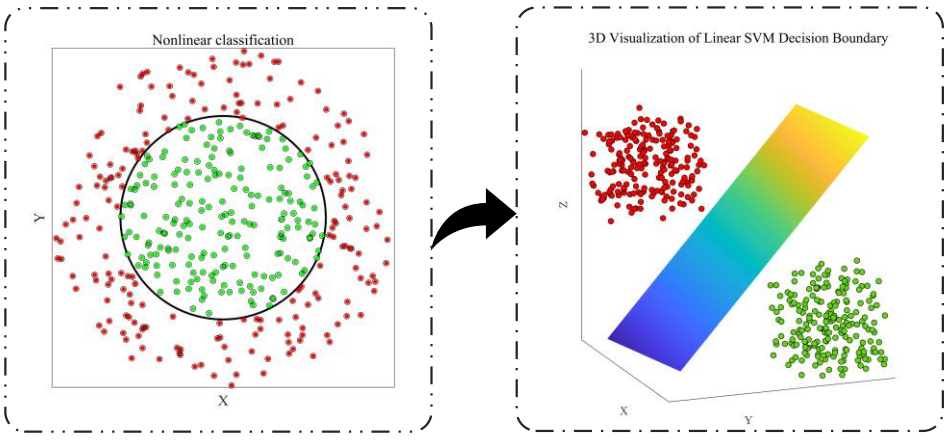

Figure 1. Relationship between samples before and after kernel function mapping.

 doi:10.20944/preprints202601.2178.v1

2.2. Dung Beetle Optimization

DBO is a recently developed metaheuristic optimization algorithm proposed by Jiankai Xue and Bo Shen [19], inspired by the foraging and reproductive behaviors of dung beetles in nature. The algorithm models multiple biologically motivated behavioral patterns—such as ball rolling, brood ball production, and foraging—to construct diverse position update strategies for population-based search. These behaviors collectively guide the search process toward promising regions of the solution space while preserving population diversity.

Distinct from conventional swarm intelligence algorithms, DBO explicitly incorporates complementary mechanisms for global exploration and local exploitation within its update framework [20]. The rolling and foraging behaviors emphasize large-scale exploration of the search space, whereas breeding-related behaviors promote local refinement around high-quality candidate solutions. This balanced search strategy enables DBO to achieve fast convergence, high solution accuracy, and improved stability in complex optimization landscapes.

Owing to its flexible search dynamics and strong optimization capability, DBO has demonstrated competitive performance in a wide range of engineering optimization problems. Its ability to adaptively adjust search behavior according to solution quality makes it particularly effective for handling nonlinear, multimodal, and constrained optimization tasks commonly encountered in real-world applications [21]. These characteristics provide a solid theoretical foundation for further enhancing the algorithm through tailored improvement strategies to address specific application requirements.

3. The Proposed Method

3.1. Overall Framework and Flowchart of the Proposed MIDBO-SVM Method

The overall framework of the proposed mechanical fault diagnosis method for HVCBs is illustrated in Figure 2. The framework integrates vibration signal processing, feature extraction, intelligent parameter optimization, and classification into a unified data-driven diagnosis pipeline. Its primary objective is to achieve accurate and robust fault identification by jointly leveraging discriminative frequency-domain features and an adaptive optimization–classification strategy. As shown in Figure 2, the proposed framework consists of four main stages: vibration signal acquisition and preprocessing, frequency-domain feature extraction, MIDBO-based SVM parameter optimization, and fault classification and decision-making.

First, mechanical vibration signals are collected from HVCBs under different operating conditions. These raw signals are preprocessed to eliminate irrelevant noise and ensure signal integrity, providing reliable inputs for subsequent analysis. Given the strong correlation between vibration characteristics and mechanical health conditions, the processed signals serve as an effective representation of the operational state of the circuit breaker.

Second, frequency-domain features are extracted from the preprocessed vibration signals using the FFT. The FFT converts the time-domain vibration signals into frequency-domain representations, revealing spectral characteristics such as dominant frequencies and energy distribution. These frequency-domain features capture essential fault-related information and form the feature vectors used as inputs to the classifier.

Third, to overcome the sensitivity of SVM performance to hyperparameter selection, a multi-strategy improved dung beetle optimization (MIDBO) algorithm is employed to automatically optimize the SVM penalty parameter C and kernel parameter g. In this stage, each MIDBO individual encodes a candidate parameter pair (C, g), and the fitness of each individual is evaluated using the classification accuracy obtained through cross-validation. By integrating enhanced population initialization, adaptive search strategies, and stochastic mutation mechanisms, MIDBO efficiently explores the parameter space and converges toward the optimal parameter combination.

Finally, the SVM classifier with optimized parameters is trained using the extracted frequency-domain features and applied to identify the mechanical operating conditions and fault types of the

 doi:10.20944/preprints202601.2178.v1

high-voltage circuit breaker. The classification results provide an accurate and reliable diagnosis of the circuit breaker's mechanical state.

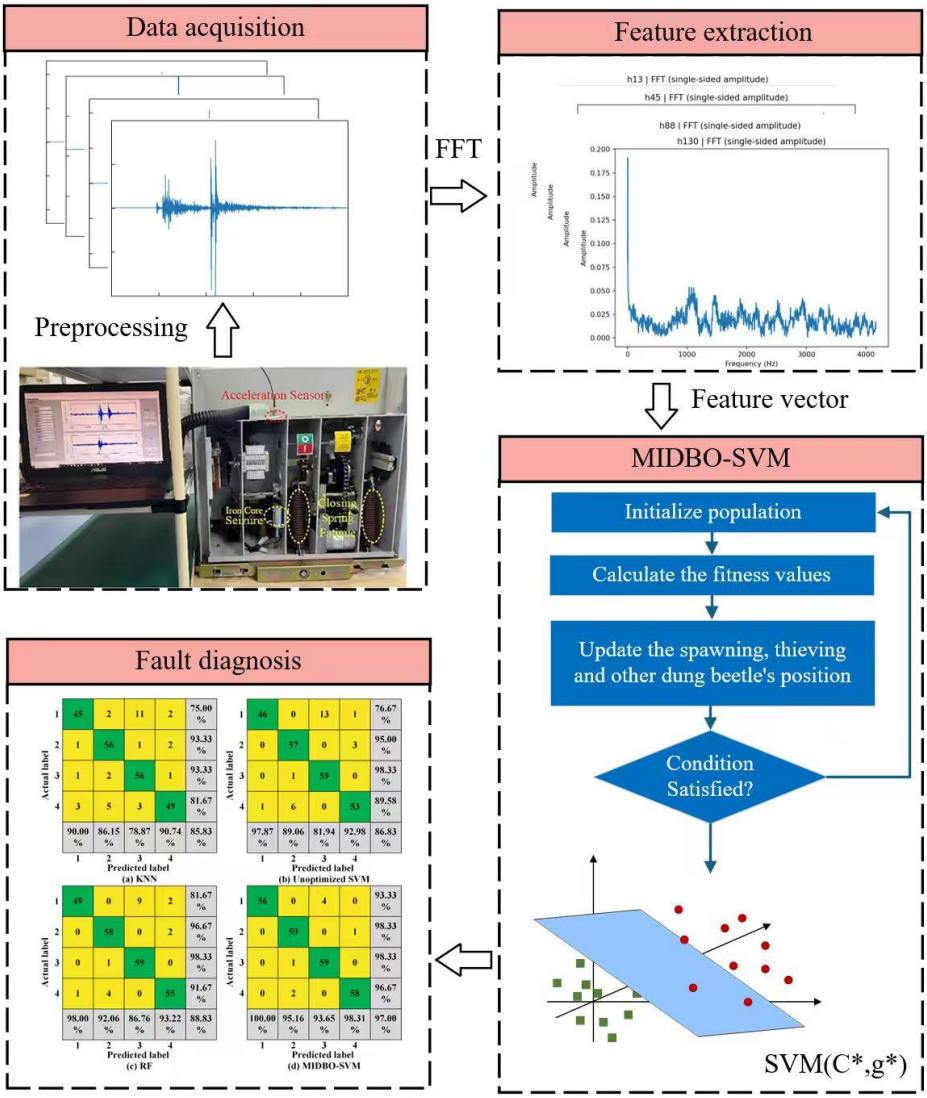

Figure 2. Flowchart of the proposed MIDBO-SVM–based mechanical fault diagnosis framework.

3.2. Multi-Strategy Improved DBO Algorithm

Although the original DBO algorithm exhibits competitive performance in global optimization, its search behavior may still suffer from several inherent limitations when applied to complex, high-dimensional, and multimodal problems, such as premature convergence, insufficient population diversity, and stagnation around local optima. To address these issues and further enhance the robustness and optimization efficiency of DBO, this study proposes a MIDBO framework. Specifically, three complementary strategies are introduced: 1) a best point set–based circular chaotic mapping strategy to enhance population diversity during initialization; 2) a sine–cosine search mechanism with random inertia weight to dynamically balance global exploration and local exploitation during the iterative process; and 3) a Cauchy–Gaussian mutation strategy to mitigate population stagnation and improve convergence accuracy in later iterations. By integrating these strategies in a coordinated manner, MIDBO significantly strengthens the global search capability, convergence stability, and solution precision of the original DBO.

 doi:10.20944/preprints202601.2178.v1

3.2.1. Best Point Set—Circular Chaotic Mapping Technique

In swarm intelligence optimization algorithms, the quality of the initial population plays a critical role in determining the subsequent search efficiency and convergence performance [30]. Conventional random initialization often leads to uneven population distribution and aggregation phenomena, which reduce population diversity and increase the likelihood of premature convergence to local optima. As a result, the global search capability of the algorithm may be severely compromised. To alleviate the uneven distribution caused by random initialization and to improve the coverage of the search space in the early evolutionary stage, a chaotic mapping–based population initialization strategy is adopted in this study [31]. Chaotic maps possess intrinsic properties such as ergodicity, randomness, and sensitivity to initial conditions, which are highly desirable for enhancing population diversity and global exploration.

Common chaotic mapping methods include logistic mapping and tent mapping. However, logistic mapping typically suffers from non-uniform distribution, which may adversely affect convergence speed and solution accuracy. Although tent mapping exhibits better uniformity, it is prone to unstable periodic cycles and fixed points. Therefore, this study employs a circle chaotic map, which demonstrates superior stability and uniform distribution characteristics, and combines it with the best point set theory to generate a high-quality initial population.

Assume that G_s denotes a unit cube in an s-dimensional Euclidean space, i.e., $x \in G_s$, where $i = 1,2,\dots,s$. If $r \in G_s$, the corresponding best point set $p_n(i)$ is defined as $p_n(i) = \{\{r_1 n_i\},\{r_2 n_i\},\cdots\{r_i n_i\}\}$ and its deviation can be expressed as shown in Equation (6).

$$\varphi(\mathrm{n}) = C(r,\varepsilon)n^{(-1+\varepsilon)}, \tag{6}$$

Here, $C(r,\varepsilon)$ is a constant related to parameters r and $\varepsilon > 0$, where r is referred to as the favorable point, defined as in Equation (10). The prime number p is the smallest integer satisfying $(p-s)/2 \geq s$, and $\{\cdot\}$ denotes the fractional part.

$$r_k = \left\{2\cos\frac{2\pi k}{p}\right\}, 1 \leq k \leq s, \tag{7}$$

The circle chaotic map is formulated as:

$$x_{i+1} = \mathrm{mod}\left(x_i + b - \left(\frac{a}{2\pi}\right)\sin(2\pi x_i), 1\right), \tag{8}$$

where $a = 0.2$ and $b = 0.5$. Compared with random initialization, the circle chaotic map significantly enhances the uniformity and spatial diversity of the population, thereby enlarging the coverage of the initial solution space and improving optimization efficiency.

Based on the above principles, the population mapping strategy adopted in this paper is described by Equation (9):

$$x_{i+1} = \begin{cases} \mathrm{mod}\left(x_i + b - \left(\frac{a}{2\pi}\right)\sin(2\pi x_i), 1\right) & , o \geq 0.7, \\ lb + \mathrm{mod}(i \times r_k, 1) \times (ub - lb), & o < 0.7 \end{cases} \tag{9}$$

where o denotes a uniformly distributed random number in the interval $[0,1]$. A visual comparison between random initialization and the proposed best point set–circle chaotic mapping is presented in Figure 3, demonstrating the superior distribution characteristics of the proposed method.

 doi:10.20944/preprints202601.2178.v1

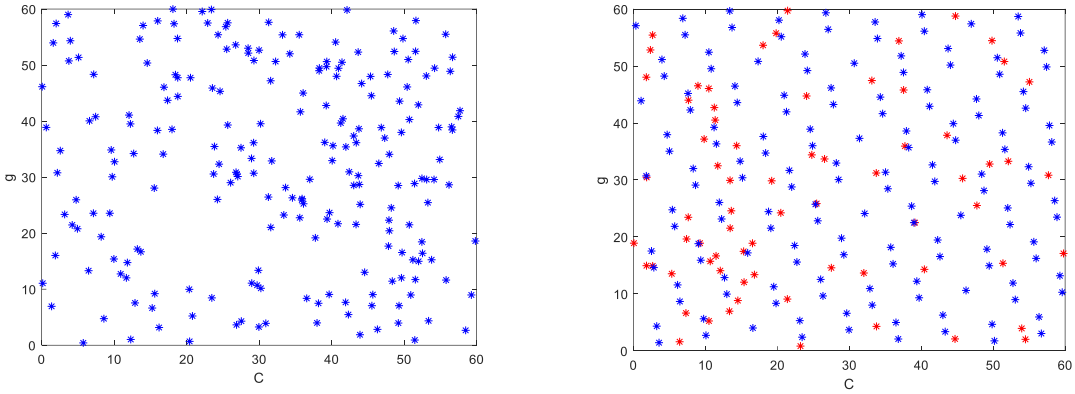

(a) population random distribution map (b) best point set - circle chaos map

Figure 3. Comparison of initialization methods: (a) population random distribution diagram and (b) best point set - circle chaos map.

3.2.2. Sine and Cosine Search Strategy Based on Random Inertia Weight

The inertia weight plays a crucial role in controlling the balance between exploration and exploitation in swarm intelligence algorithms, as it reflects an individual's tendency to preserve historical motion states. In conventional linear-decreasing inertia weight schemes, if the optimal solution is not identified in the early stage, the gradually diminishing weight may cause the population to lose exploration capability and become trapped in local optima. To overcome this drawback, a sine–cosine search strategy combined with a random inertia weight is introduced to update the position of producer dung beetles [32]. The sine–cosine mechanism enables individuals to approach the global optimum in an oscillatory manner, effectively preventing overly aggressive convergence. Meanwhile, the stochastic inertia weight dynamically adjusts the influence of previous states, thereby enhancing adaptability throughout the optimization process.

The position update formulas are given by Eqs. (10) and (11):

$$x_i(t+1)=\begin{cases}\omega x_i(t)+r_1\times\sin(r_0)\times(\alpha\times \mathrm{k}\times x_i(t-1)+b\times\Delta x), \lambda<0.8\\ \omega x_i(t)+r_0\times\cos(r_1)\times\tan(\theta)\left|x_i(t)-x_i(t-1)\right|, \lambda\geq 0.8\end{cases}, \tag{10}$$

$$\omega=\omega_{max}+\left(\omega_{max}-\omega_{min}\right)\bullet rand()+\delta\bullet randn();, \tag{11}$$

where $w_{\max}=0.9$ and $w_{\min}=0.4$ denote the upper and lower bounds of the inertia weight, respectively. The function $rand()$ generates a uniformly distributed random number in $[0,1]$, while $randn()$ represents a standard normal random variable. The parameter σ quantifies the deviation between the stochastic inertia weight and its expected value and is set to 0.3 in this study.

By integrating sine–cosine oscillatory guidance with adaptive inertia adjustment, the proposed strategy effectively balances global exploration and local exploitation, significantly reducing the risk of premature convergence.

3.2.3. Cauchy–Gaussian Mutation Strategy

In the later stages of DBO iterations, rapid population convergence may lead to stagnation near local optima, limiting further performance improvement. To address this issue, a Cauchy–Gaussian mutation strategy is introduced to enhance population diversity and refine local search accuracy [33].

Gaussian mutation perturbs an individual by adding a random vector following a Gaussian distribution. The one-dimensional Gaussian probability density function with mean μ and variance σ is given by Equation (12):

 doi:10.20944/preprints202601.2178.v1

$$f_G(\mathrm{x}) = \frac{1}{\sigma\sqrt{2\pi}} e^{-\frac{(x-\mu)^2}{2\delta^2}}, -\infty < x < \infty, \tag{12}$$

In contrast, the Cauchy distribution, whose probability density function is shown in Equation (13), exhibits heavier tails and can generate larger perturbations, which are particularly beneficial for escaping local optima:

$$f_C(\mathrm{x}) = \frac{1}{\pi} \bullet \frac{t}{x^2 + t^2}, -\infty < x < \infty, \tag{13}$$

In this study, the Cauchy–Gaussian mutation strategy is applied to the best-performing individuals. A competitive selection mechanism is employed to retain the solution with superior fitness after mutation. The corresponding update rules are defined in Eqs. (14)–(16), where P_{gbest} represents the mutated best position, X_{gbest} denotes the original global best individual, and X_{newbest} is the updated optimal solution. The parameter σ^2 is the standard deviation of the mutation, while λ_1 and λ_2 are adaptive coefficients that vary with iteration count.

$$P_{gbest} = X_{gbest}\left[1 + \lambda_1 Cauchy(0,\sigma^2) + \lambda_2 Gauss(0,\sigma^2)\right], \tag{14}$$

$$X_{newbest} = \begin{cases} P_{\mathrm{gbest}}, f(P_{\mathrm{gbest}}) < f(X_{\mathrm{gbest}}) \\ X_{\mathrm{gbest}}, \mathrm{otherwise} \end{cases}, \tag{15}$$

$$\begin{cases} \lambda_1 = 1 - \dfrac{t^2}{T^2} \\ \lambda_2 = \dfrac{t^2}{T^2} \end{cases}, \tag{16}$$

At the early stage of optimization, larger values of λ_1 amplify the influence of Cauchy mutation, facilitating extensive global exploration. As iterations proceed, λ_1 gradually decreases and λ_2 increases, shifting the mutation behavior toward Gaussian perturbation to enhance local refinement and convergence precision. Through this adaptive mechanism, the complementary advantages of Cauchy and Gaussian distributions are effectively exploited, achieving a robust balance between exploration and exploitation.

3.3. MIDBO–SVM Parameter Optimization Modeling

SVM has demonstrated strong generalization ability and robustness in small-sample and nonlinear classification problems, making it well suited for mechanical fault diagnosis of HVCBs. However, the diagnostic performance of SVM is highly sensitive to its hyperparameters, particularly the penalty parameter *C* and the kernel parameter *g* of the RBF [34]. Inappropriate parameter settings may lead to overfitting, underfitting, or poor generalization capability. Therefore, an efficient and reliable parameter optimization strategy is essential for fully exploiting the classification potential of SVM. In this study, the proposed MIDBO algorithm is employed to automatically search for the optimal combination of SVM parameters. As illustrated in Figure 1, MIDBO–SVM integrates feature-driven model training with evolutionary optimization, forming a closed-loop diagnosis framework that links signal processing, intelligent optimization, and fault classification.

3.3.1. Optimization Objective and Fitness Function Design

The goal of MIDBO–SVM parameter optimization is to identify the optimal hyperparameter pair:

$$\Theta = \{C, g\}, \tag{16}$$

 doi:10.20944/preprints202601.2178.v1

which maximizes the classification performance of the SVM model on mechanical vibration feature data.

To ensure robust performance evaluation and avoid overfitting, k-fold cross-validation accuracy is adopted as the fitness function. For each candidate solution Θ_i, the fitness value is defined as:

$$Fitness(\Theta_i) = \frac{1}{k}\sum_{j=1}^{k} \mathrm{Acc}_j , \tag{17}$$

where Acc_j denotes the classification accuracy obtained on the j-th validation fold, and k represents the number of folds. This fitness formulation provides a reliable estimate of generalization ability and ensures fair comparison among candidate solutions.

The optimization problem can thus be formulated as:

$$\max_{\Theta} Fitness(C, g), \tag{18}$$

subject to

$$C_{\min} \le C \le C_{\max}, g_{\min} \le g \le g_{\max}, \tag{19}$$

where $[C_{\min}, C_{\max}]$ and $[\gamma_{\min}, \gamma_{\max}]$ define the feasible search ranges.

3.3.2. Encoding Strategy and Search Space Construction

Within the MIDBO framework, each dung beetle individual represents a candidate SVM parameter solution, encoded as a two-dimensional position vector:

$$X_i = \{C_i, g_i\}, \tag{20}$$

The initial population is generated using the best point set–circle chaotic mapping strategy introduced in Section 3.2.1, ensuring uniform coverage of the parameter search space and enhanced population diversity. This initialization mechanism allows MIDBO to explore a wide range of parameter combinations from the early stage, reducing sensitivity to initial conditions.

3.3.3. MIDBO-Driven Evolutionary Optimization Process

During the optimization process, the MIDBO algorithm iteratively updates the positions of dung beetle individuals based on the multi-strategy enhancement mechanisms described in Section 3.2. Specifically: 1) Global exploration stage: the sine–cosine search strategy with random inertia weight guides individuals to explore the parameter space in an oscillatory and adaptive manner, preventing premature convergence and encouraging exploration of promising regions. 2) Adaptive transition stage: as iterations proceed, the adaptive inertia mechanism dynamically balances exploration and exploitation, allowing the population to gradually concentrate around high-fitness regions in the parameter space. 3) Local refinement stage: the Cauchy–Gaussian mutation strategy is applied to elite individuals to introduce controlled perturbations. Cauchy mutation enhances the ability to escape local optima, while Gaussian mutation improves fine-grained local search precision, leading to stable convergence.

At each iteration, the fitness of all candidate solutions is evaluated using cross-validation accuracy, and the global best solution is updated accordingly. The iterative process continues until the termination condition—maximum number of iterations or convergence criterion—is satisfied.

3.3.4. Optimal SVM Model Construction and Fault Classification

Upon completion of the MIDBO optimization process, the optimal parameter set $\Theta^* = \{C^*, g^*\}$ is obtained. These parameters are then used to construct the final SVM classifier.

 doi:10.20944/preprints202601.2178.v1

The optimized SVM model is trained using the FFT-based frequency-domain feature vectors extracted from mechanical vibration signals and subsequently applied to identify the operating states and fault types of HVCBs. As shown in Figure 1, this process completes the full diagnostic pipeline, from signal acquisition and feature extraction to intelligent optimization and fault decision-making. By tightly coupling MIDBO with SVM parameter tuning, the proposed method significantly enhances classification accuracy, convergence stability, and robustness under unbalanced sample conditions, thereby providing a reliable and efficient solution for mechanical fault diagnosis of HVCBs.

3.4. MIDBO–SVM Fault Diagnosis Procedure

To fully exploit the parameter optimization capability of the proposed MIDBO algorithm, a structured MIDBO–SVM fault diagnosis procedure is established for HVCBs. The overall workflow of the proposed method is illustrated in Figure 4, where vibration signal processing, evolutionary parameter optimization, and fault classification are tightly integrated.

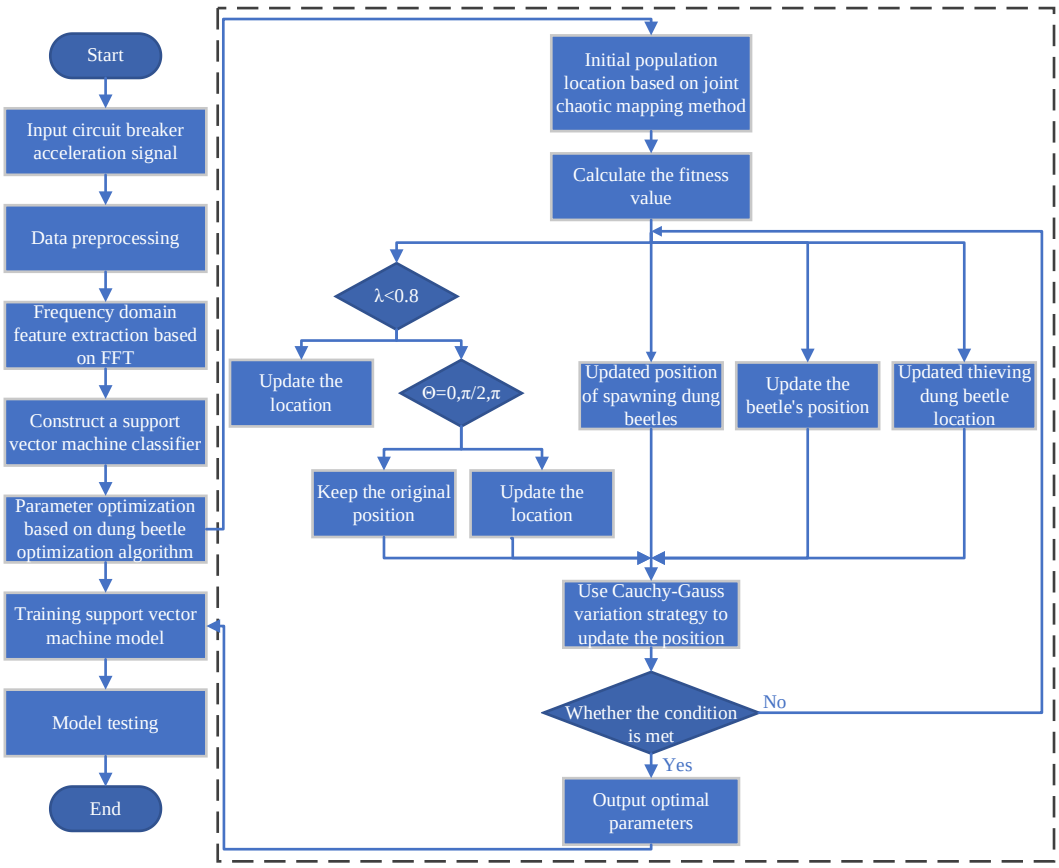

Figure 4. Flowchart of the HVCB fault diagnosis based on the MIDBO-SVM model.

The detailed fault diagnosis procedure is described as follows:

(1) Initialization of Algorithm Parameters

The initial settings of the MIDBO–SVM framework are defined, including the maximum number of iterations, population size, search dimension, search ranges of the SVM hyperparameters C and g, inertia weight parameters, and mutation-related coefficients. These settings determine the search boundaries and evolutionary dynamics of the MIDBO algorithm.

(2) Population Initialization and Fitness Evaluation

The initial population is generated using the best point set–circle chaotic mapping strategy according to Equation (9), ensuring a uniform and diverse distribution of candidate solutions within the parameter space.

 doi:10.20944/preprints202601.2178.v1

Each dung beetle individual encodes a candidate SVM hyperparameter pair (C, g). For each individual, an SVM classifier is constructed and evaluated using cross-validation accuracy on the extracted frequency-domain features. The fault diagnosis error rate is adopted as the fitness criterion. Based on the fitness values, the individual best solutions and the global best solution are identified and recorded.

(3) Evolutionary Update and Global Best Tracking

During each iteration, the positions of dung beetle individuals are updated according to the MIDBO evolutionary rules described in Section 3.2. The fitness of the updated population is re-evaluated, and the historical best positions as well as the global optimal solution are updated through fitness comparison. This process guides the population toward high-quality parameter regions while maintaining an effective balance between global exploration and local exploitation.

(4) Cauchy–Gaussian Mutation and Competitive Selection

To prevent premature convergence and enhance population diversity, the Cauchy–Gaussian mutation strategy is applied to elite individuals following Equation (14). The fitness values before and after mutation are compared, and the solution with superior fitness is retained as the optimal candidate for the current iteration. This competitive selection mechanism ensures that beneficial perturbations are preserved in the evolutionary process.

(5) Termination Judgment and Optimal Parameter Output

The algorithm evaluates whether the maximum iteration number has been reached. If the termination condition is not satisfied, the iteration index is updated (t=t+1), and the procedure returns to Step 2. Otherwise, the optimization process terminates, and the optimal SVM hyperparameter combination (C^*, g^*) is obtained.

(6) Fault Classification Using Optimized SVM

Finally, the optimized SVM classifier constructed with (C^*, g^*) is employed to identify the operating conditions and mechanical fault types of HVCBs. This step completes the fault diagnosis workflow illustrated in Figure 3.

4. Data Acquisition

To evaluate the effectiveness and engineering applicability of the proposed MIDBO–SVM fault diagnosis method, an experimental fault simulation platform was constructed using a VS1 HVCB as the research object. The training and testing datasets were obtained by simulating typical mechanical operating conditions and representative fault scenarios of the circuit breaker. The schematic diagram and physical configuration of the data acquisition system are shown in Figure 5 [35].

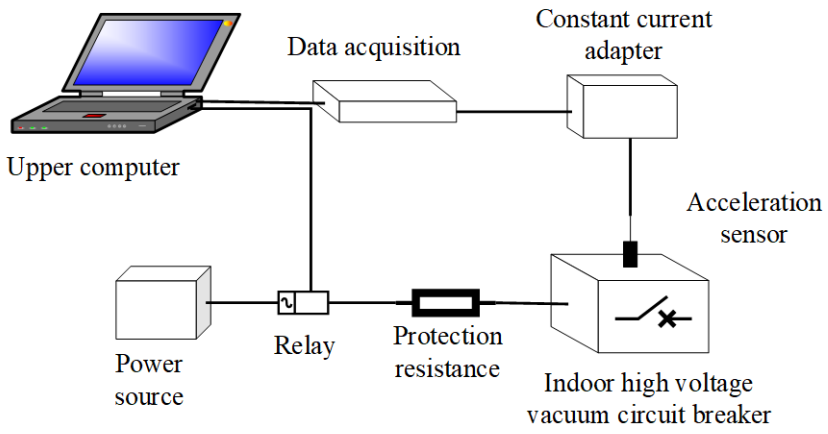

(**a**) Schematic diagram of signal acquisition system

 doi:10.20944/preprints202601.2178.v1

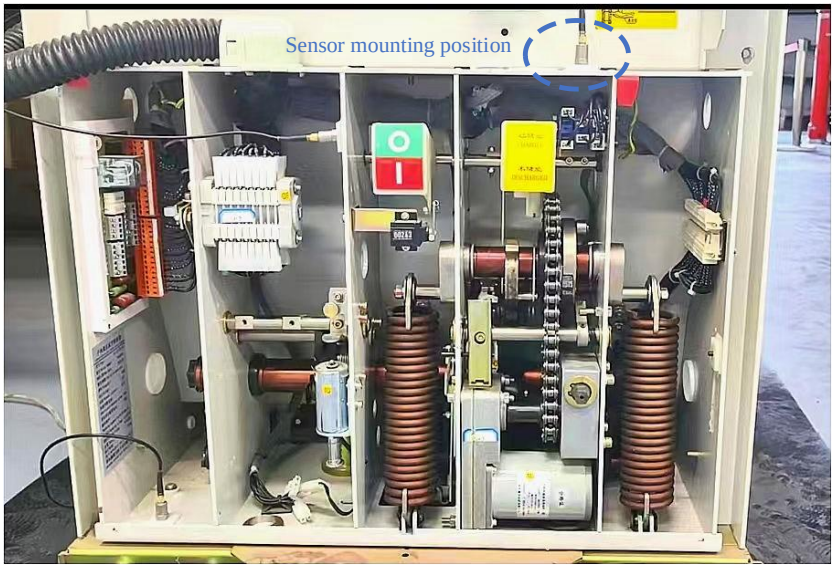

(**b**) Experimental equipment

Figure 5. Data acquisition system diagram: (a) schematic diagram of signal acquisition system and (b) experimental equipment.

During the experiments, mechanical vibration signals generated by the circuit breaker operating mechanism were collected using acceleration sensors and transmitted to an industrial computer through a high-speed data acquisition card. The acquired signals were stored and monitored in real time, providing a reliable basis for subsequent feature extraction and fault diagnosis.

The VS1 HVCB is an indoor vacuum circuit breaker widely used in 12-kV power distribution systems. It integrates a spring-operated mechanism with the circuit breaker body and operates at a rated frequency of 50 Hz with a rated current of 1600 A. During opening and closing operations, the rapid release of spring energy causes intensive metal-to-metal impacts among internal mechanical components. These impacts generate broadband vibration signals, with significant frequency components extending beyond 20 kHz, particularly during the closing process. Therefore, sensors with high-frequency response characteristics are required to accurately capture the vibration information associated with mechanical conditions.

In this study, a CT1000L piezoelectric acceleration sensor with a sensitivity of 5 mV/g was selected to ensure accurate measurement of transient vibration signals. To improve signal fidelity and frequency response, the sensor was mounted on the beam of the circuit breaker operating mechanism, which exhibits strong vibration transmission characteristics. The sensor was firmly fixed using a combination of industrial adhesive and mechanical bolts to ensure a level contact surface and stable installation, thereby reducing signal attenuation and external interference.

The vibration signals were acquired using an NI USB-6002 data acquisition card, which provides a maximum sampling rate of 50 kS/s and a 16-bit resolution. Under no-load closing conditions, the operating mechanism of the VS1 circuit breaker typically completes its motion within 35–70 ms. To ensure complete capture of transient vibration characteristics while maintaining computational efficiency, the acquisition duration was set to 1 s, and the sampling frequency was configured at 10 kHz.

Four typical operating conditions of the circuit breaker under no-load closing states were investigated in this study, including one normal condition and three representative mechanical fault conditions: iron core sticking, loose transmission guide rod, and loose base bolt. The iron core sticking fault was simulated by inserting a spring into the iron core to increase surface resistance, mimicking adhesion caused by contamination or wear. The loose transmission guide rod fault was reproduced by loosening the transmission mechanism screw by approximately 3 mm, representing mechanical degradation due to long-term operation. The loose base bolt fault was simulated by loosening the

 doi:10.20944/preprints202601.2178.v1

four mounting bolts at the base of the circuit breaker, which reduces structural stability and alters vibration transmission paths.

For each operating condition, vibration acceleration signals were repeatedly collected to ensure statistical reliability. The vibration waveforms obtained under normal and faulty conditions are illustrated in Figure 6. These datasets form the experimental foundation for validating the proposed MIDBO–SVM fault diagnosis framework in terms of classification accuracy, robustness, and generalization performance.

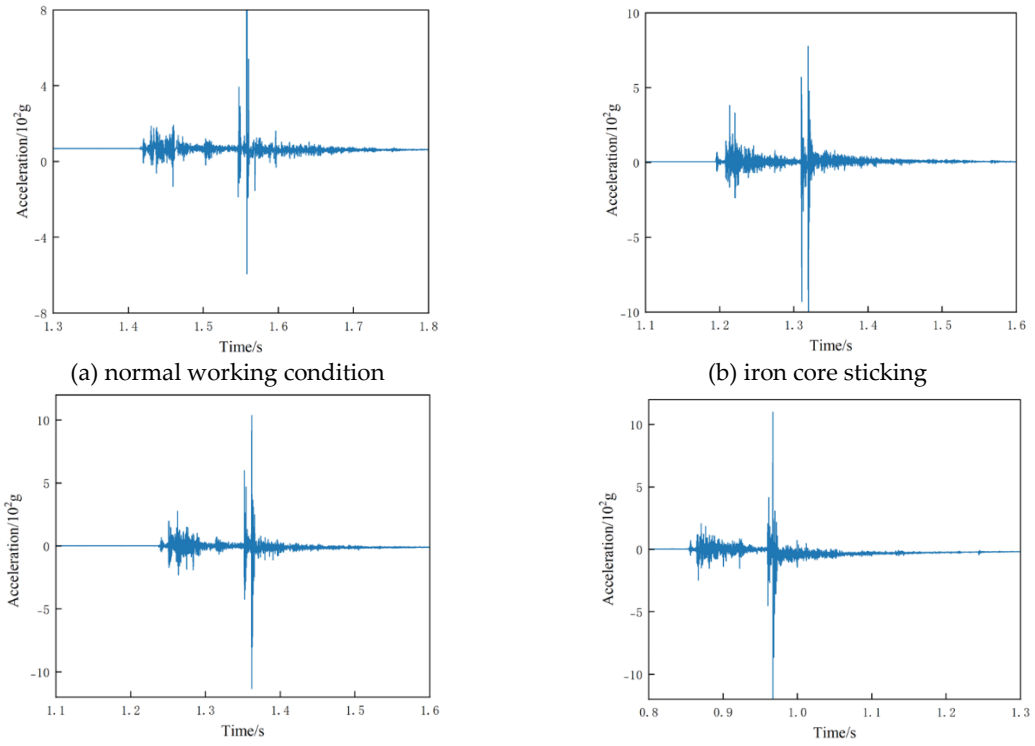

(a) normal working condition (b) iron core sticking

(c) loose transmission guide rod (d) loose base bolt

Figure 6. Four vibration signals: (a) normal working condition, (b) iron core sticking, (c) loose transmission guide rod and (d) loose base bolt.

5. Results and Analysis

In this study, FFT was employed to extract frequency-domain features from both training and test samples, which were subsequently used as inputs to the support vector machine (SVM) classifier. To mitigate the sensitivity of SVM performance to hyperparameter selection, the proposed MIDBO algorithm was adopted to optimize the penalty factor C and kernel parameter g. To ensure fair comparison, all optimization-based classifiers were trained and evaluated using identical datasets, feature extraction procedures, and parameter search ranges. The population size and maximum iteration number for all optimization algorithms were set to 30, with $C \in [0,60]$ and $g \in [0,60]$.

The population evolution processes of different optimization methods are illustrated in Figure 7. It can be observed that the whale optimization algorithm (WOA) exhibits limited population diversity during the later stages of optimization, which leads to premature convergence and stagnation. Although WOA converges relatively quickly, its restricted global search capability limits further performance improvement. The PSO method demonstrates a highly stochastic search trajectory with evident randomness in the distribution of candidate solutions. As the optimization progresses, the population diversity of PSO decreases rapidly, increasing the likelihood of being trapped in local optima. Consequently, PSO-SVM often requires repeated experiments to obtain acceptable solutions and suffers from slow convergence and low optimization precision.

Compared with PSO and WOA, the DBO algorithm shows a more uniform population distribution and improved global exploration ability, as illustrated in Figure 7(c). However, its local

 doi:10.20944/preprints202601.2178.v1

exploitation capability remains insufficient, resulting in convergence toward suboptimal solutions in some cases. By contrast, the proposed MIDBO algorithm effectively overcomes these limitations. Through an improved population initialization strategy and adaptive regulation of inertia weight ω and dynamic parameters, MIDBO achieves a better balance between global exploration and local exploitation. The real-time adjustment of population movement enables the algorithm to follow a coarse-to-fine optimization strategy, significantly improving convergence speed, stability, and solution accuracy.

The convergence behaviors of the four optimization algorithms are further compared in Figure 8. The PSO-SVM model exhibits alternating stagnation and re-search phenomena during optimization and converges to an error value of 0.1042 after 14 iterations, indicating limited optimization capability. Although WOA-SVM converges faster than PSO-SVM, its final accuracy improvement is marginal, suggesting insufficient local search refinement. The DBO-SVM model achieves better convergence accuracy and speed than the two aforementioned methods; however, the imbalance between its exploration and exploitation abilities remains evident. In contrast, the proposed MIDBO-SVM reaches an error rate of 0.0333 within only three iterations, achieving the highest convergence accuracy with the fewest iterations. This demonstrates that MIDBO significantly enhances the optimization efficiency and robustness of SVM hyperparameter tuning while reducing the probability of convergence to local optima.

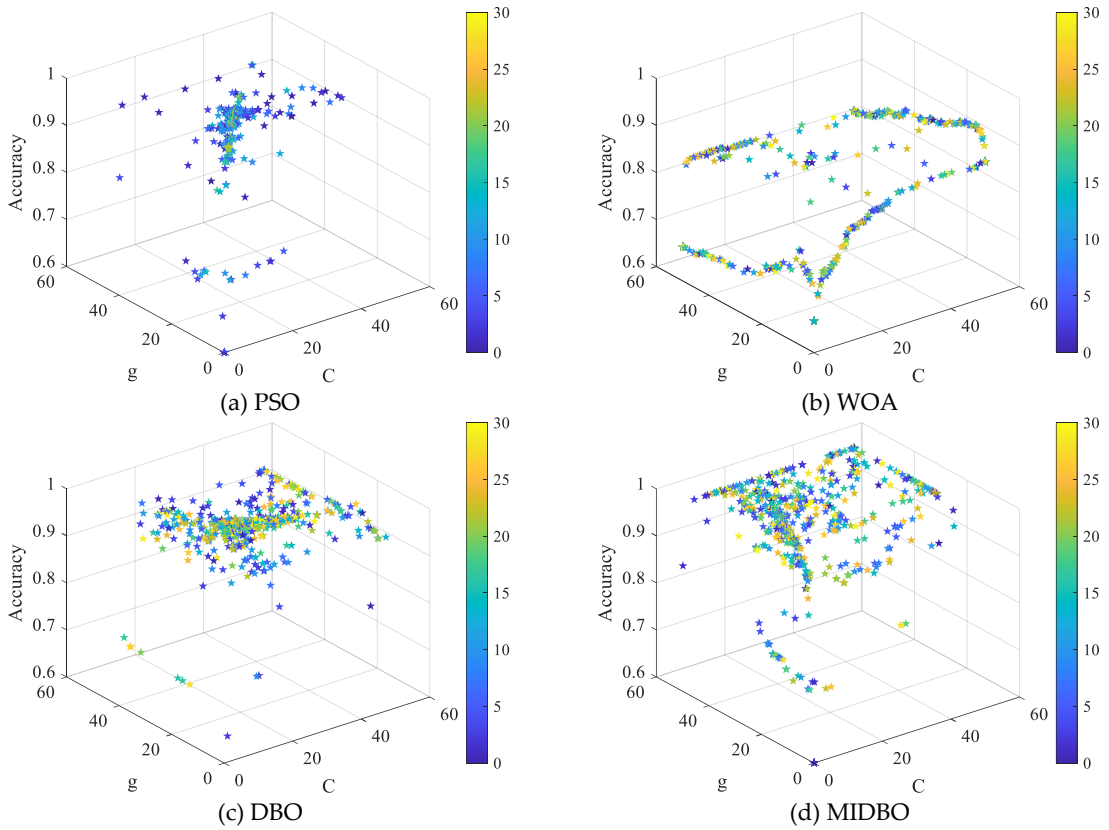

Figure 7. Spatial distribution of parameter optimization: (a) PSO-SVM method, (b) WOA-SVM method, (c) DBO-SVM method and (d) MIDBO-SVM method.

 doi:10.20944/preprints202601.2178.v1

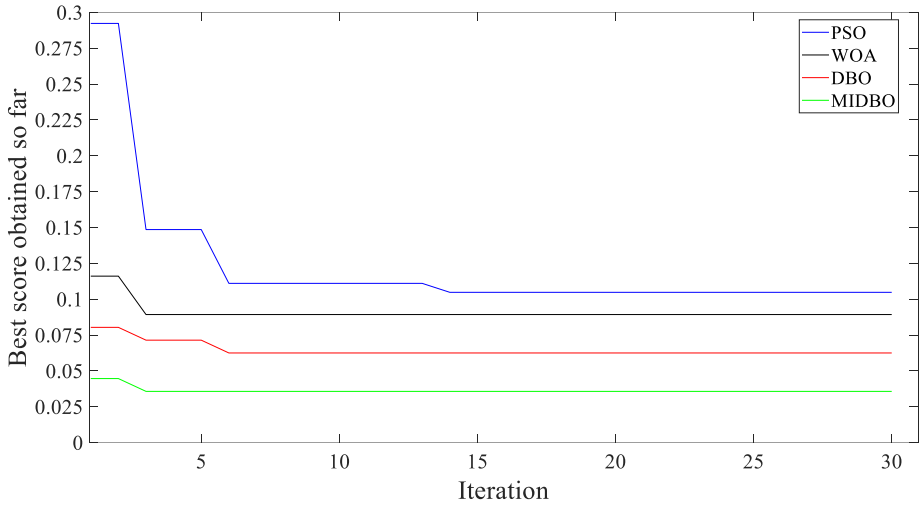

Figure 8. Iterative convergence curves of the four parameter optimization methods.

The fault diagnosis performance of different optimized SVM models is summarized in Table 1. The four operating conditions—normal condition, iron core adhesion, slack transmission guide rod, and loose base bolts—correspond to Classes 1–4, respectively. Among all compared methods, MIDBO-SVM achieves the highest overall diagnostic accuracy of 96.67%. For fault Classes 2 and 3, all optimized methods achieve accuracies above 95%, indicating that these fault patterns are relatively distinguishable in the feature space. However, for Class 1 (normal condition) and Class 4 (loose base bolts), which exhibit higher similarity and are more prone to misclassification, MIDBO-SVM demonstrates obviously advantages. Specifically, the diagnostic accuracy of MIDBO-SVM for Class 1 reaches 93.3%, exceeding those of WOA-SVM, PSO-SVM, and DBO-SVM by 15.0%, 17.0%, and 8.3%, respectively. For Class 4, MIDBO-SVM achieves an accuracy of 96.7%, outperforming the other three methods by 6.7%, 11.7%, and 3.4%, respectively. These results indicate that MIDBO-SVM possesses stronger discriminative capability for subtle mechanical fault features and demonstrates superior global optimization performance.

Table 1. Comparison of diagnosis outcomes for different fault types.

Model	Actual class	Prediction class				Accuracy
		1	2	3	4	
WOA	1	47	0	12	1	91.25%
	2	0	59	0	1	
	3	0	1	59	0	
	4	1	5	0	54	
PSO	1	46	0	13	1	89.58%
	2	0	57	0	3	
	3	0	1	59	0	
	4	1	6	0	53	
DBO	1	51	0	8	1	93.75%
	2	0	59	0	1	
	3	0	1	59	0	
	4	0	4	0	56	
MIDBO	1	56	0	4	0	96.67%
	2	0	59	0	1	
	3	0	1	59	0	
	4	0	2	0	58	

 doi:10.20944/preprints202601.2178.v1

To further evaluate the effectiveness of the proposed MIDBO-SVM approach, additional comparisons were conducted with several widely used conventional classification methods, including an unoptimized SVM, k-nearest neighbors (KNN), and random forest (RF). All classifiers were implemented using identical FFT-based feature representations and the same training–testing data partitions to ensure a fair comparison. The quantitative results in terms of average classification accuracy and standard deviation (Std) obtained over multiple independent runs are summarized in Table 2. As shown in Table 2, the unoptimized SVM achieves an overall accuracy of 86.25%, which is notably lower than that of the proposed MIDBO-SVM. This result clearly demonstrates that inappropriate hyperparameter selection can severely degrade SVM classification performance, even when informative frequency-domain features are employed. The KNN classifier exhibits the lowest accuracy and the largest standard deviation, indicating limited generalization capability and high sensitivity to sample distribution variations. Although RF outperforms both KNN and the unoptimized SVM by leveraging ensemble learning, its diagnostic accuracy and stability remain inferior to those of MIDBO-SVM. Notably, MIDBO-SVM not only achieves the highest average accuracy but also exhibits the smallest std among all compared methods, indicating superior robustness and repeatability. This performance gain confirms that the proposed multi-strategy optimization mechanism enables the SVM to converge consistently toward high-quality hyperparameter configurations, thereby enhancing both classification precision and stability.

Table 2. Performance comparison of conventional classifiers and MIDBO-SVM.

Methods	Diagnosis accuracy (%)	
	Accuracy	Std
KNN	84.55	3.41
Unoptimized SVM	86.25	2.87
RF	89.17	2.14
MIDBO-SVM	96.67	0.94

To further investigate the diagnostic behavior of different classifiers, confusion matrix analysis was conducted, with particular emphasis on the misclassification of normal operating conditions, which is a critical concern in practical condition monitoring systems. The confusion matrices of the representative classifiers are reported in Figure 9, where Class 1 corresponds to normal operation and Class 4 represents the loose base bolt fault, which exhibits feature characteristics partially overlapping with normal conditions. The confusion matrix results reveal that conventional classifiers, particularly the unoptimized SVM and RF, tend to misclassify normal operating samples as loose base bolt faults. This misclassification arises from overlapping vibration frequency features between healthy states and early-stage mechanical looseness, leading to blurred decision boundaries. Such false alarms are highly undesirable in real-world applications, as they may trigger unnecessary maintenance actions and reduce system reliability. In contrast, the proposed MIDBO-SVM significantly reduces the misclassification of normal samples, achieving the highest true positive rate for Class 1 while simultaneously maintaining high precision for fault categories. This improvement indicates that the MIDBO-optimized SVM constructs a more discriminative and compact decision boundary, effectively separating normal conditions from fault states with similar spectral characteristics. Overall, the confusion matrix analysis confirms that MIDBO-SVM not only enhances overall diagnostic accuracy but also substantially improves reliability by minimizing false fault alarms under normal operating conditions, which is essential for practical deployment in high-voltage circuit breaker condition monitoring systems.

In practical applications, HVCBs operate predominantly under normal conditions, and fault samples are scarce. To simulate this realistic scenario, unbalanced datasets were constructed, as shown in Table 3, by gradually reducing the sample sizes of Classes 1 and 4. The diagnostic results under unbalanced conditions are illustrated in Figure 10. As the degree of imbalance increases, the diagnostic accuracy of all models decreases, with PSO-SVM and WOA-SVM exhibiting particularly

 doi:10.20944/preprints202601.2178.v1

severe performance degradation due to their susceptibility to local optima under limited data conditions. In contrast, MIDBO-SVM consistently maintains high diagnostic accuracy, remaining above 86.25% even under severely unbalanced sample distributions. This robustness demonstrates that the optimized hyperparameters obtained by MIDBO endow the SVM classifier with strong generalization ability, making it more suitable for practical fault diagnosis scenarios characterized by limited and imbalanced data.

Table 3. Experimental sample data set.

Label	Dataset			
	data set 1	data set 2	data set 3	data set 4
1	50	40	30	20
2	50	50	50	50
3	50	50	50	50
4	50	40	30	20

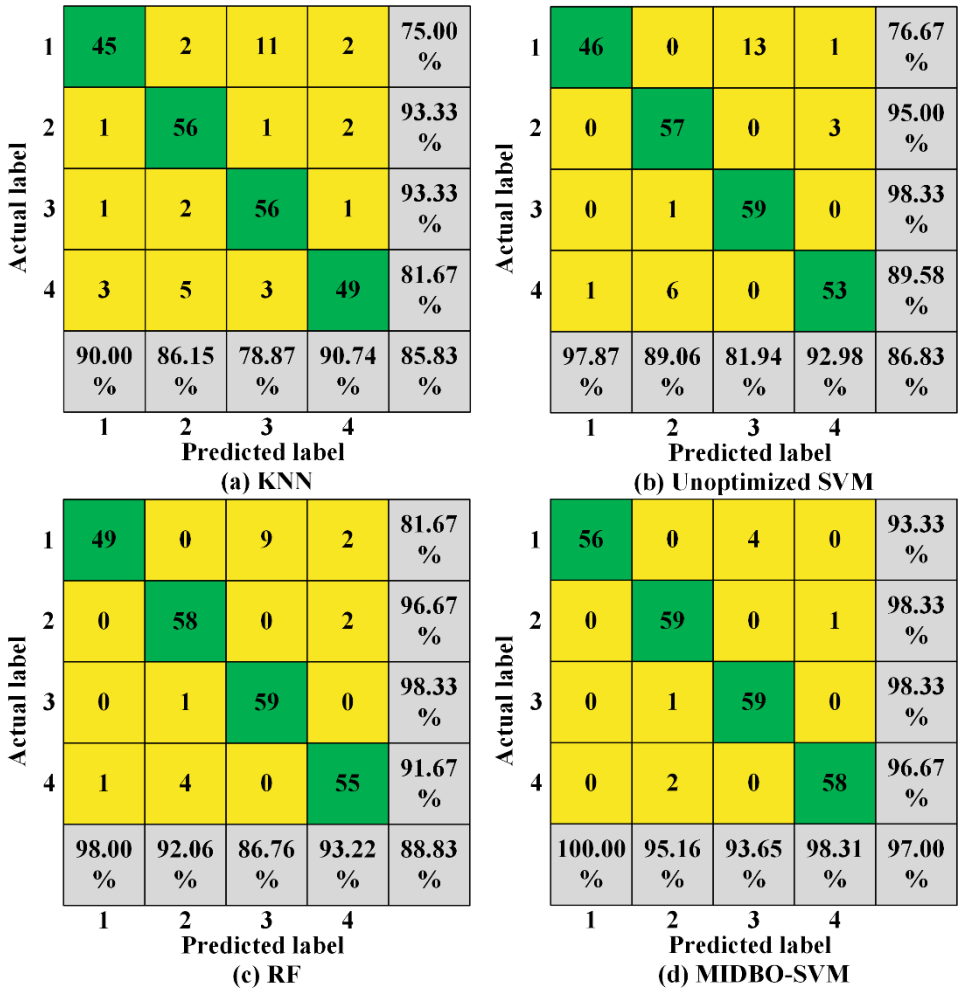

Figure 9. Confusion matrices of different classifiers.

 doi:10.20944/preprints202601.2178.v1

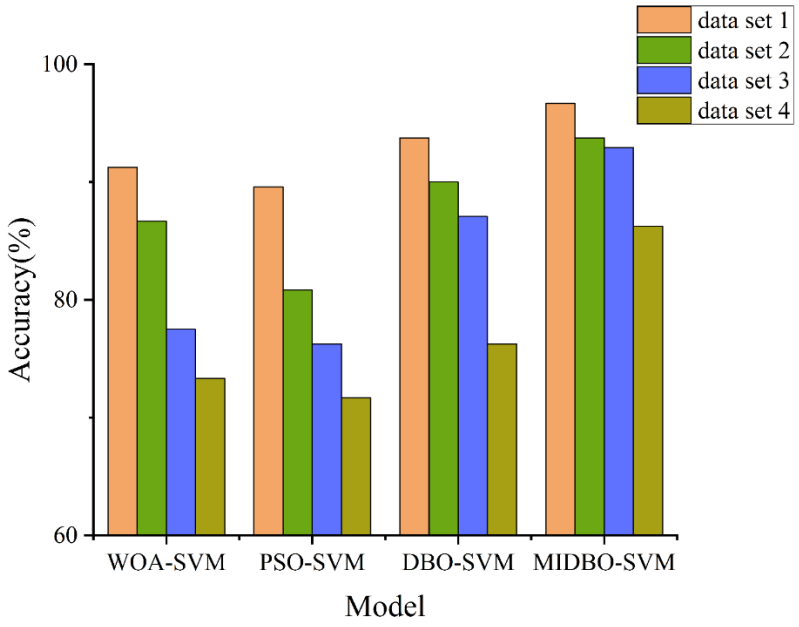

Figure 10. Fault identification results for unbalanced datasets.

From a computational perspective, the overall complexity of the proposed MIDBO-SVM framework is dominated by the optimization-based hyperparameter search and SVM training process. Let N denote the population size, M denote the number of iterations, and T_{SVM} denote the training cost of a single SVM model. The computational complexity of MIDBO-SVM can be approximated as $O(N \times M \times T_{\mathrm{SVM}})$, which is comparable to that of PSO-SVM, WOA-SVM, and DBO-SVM. However, due to its faster convergence behavior, MIDBO requires significantly fewer effective iterations to reach optimal solutions. In practice, MIDBO-SVM converges within only three iterations, whereas the other methods require more than ten iterations to stabilize. Consequently, the actual time cost of MIDBO-SVM is lower despite similar theoretical complexity. Moreover, once the optimal hyperparameters are obtained, the online fault diagnosis stage involves only standard SVM inference, which incurs negligible computational overhead. Therefore, the proposed MIDBO-SVM achieves a favorable trade-off between diagnostic accuracy and computational efficiency, demonstrating strong potential for real-time condition monitoring and fault diagnosis of HVCBs.

6. Conclusions

This paper presented a mechanical fault diagnosis framework for HVCBs based on a support vector machine optimized by a MIDBO-SVM. FFT-based frequency-domain features were extracted from vibration signals corresponding to multiple operating states, providing effective characterization of mechanical condition variations. By enhancing the original DBO with diversified population initialization, adaptive search control, and hybrid mutation strategies, the proposed MIDBO significantly improved global exploration capability, convergence speed, and optimization stability. As a result, the optimal SVM hyperparameters were reliably identified, leading to superior classification performance. Experimental results demonstrated that the proposed MIDBO-SVM achieved the highest diagnostic accuracy of 96.67% and maintained strong robustness under imbalanced sample conditions, with an accuracy of 86.25%. Compared with conventional classifiers and non-optimized SVMs, the proposed method effectively reduced misclassification of normal operating conditions and mechanically similar fault states, confirming its strong generalization capability and practical applicability. These results indicate that the proposed framework provides an effective and reliable solution for HVCB mechanical fault diagnosis and condition assessment.

 doi:10.20944/preprints202601.2178.v1

Future work will focus on extending the proposed framework toward online and real-time fault diagnosis by incorporating streaming vibration data and adaptive model updating mechanisms. In addition, multi-sensor fusion strategies combining vibration, current, and acoustic signals will be investigated to further enhance diagnostic reliability under complex operating conditions. Transfer learning and domain adaptation techniques will also be explored to improve model scalability and enable rapid deployment across different circuit breaker types and operating environments with limited labeled fault data.

Author Contributions: Conceptualization, M.L. and S.Y.; methodology, M.L.; software, A.Z.; validation, A.Z., J.G. and J.Y.; formal analysis, G.U.; investigation, S.F., A.Z. and A.Z.; resources, J.Y.; data curation, M.L.; writing—original draft preparation, M.L.; writing—review and editing, J.Y.; visualization, A.Z.; supervision, J.W.; project administration, M.L.; funding acquisition, S.Y. All authors have read and agreed to the published version of the manuscript.

Funding: This research was funded by the science and technology project funded by State Grid Jiangxi Electric Power Company, grant number 5218D0250003.

Data Availability Statement: Data is contained within the article or supplementary material.

Conflicts of Interest: The authors declare no conflicts of interest.

References

1. Ma L., et al. Mechanical Fault Diagnosis of High-Voltage Circuit Breakers Based on IPSO-VMD and KFCM-SVM. *IEEJ Transactions on Electrical and Electronic Engineering*, 2025, 20 (8), 1195-1202.
2. Yang Q., Liao Y., Li J., et al. Cross-domain zero-shot learning for enhanced fault diagnosis in high-voltage circuit breakers. *Neural Networks*, 2024, 180, 106681.
3. Yang M., et al. Research on Fault Diagnosis of High-Voltage Circuit Breakers Using Gramian-Angular-Field-Based Dual-Channel Convolutional Neural Network. *Energies*, 2025,18 (14), 3837.
4. Razi-Kazemi A.A., Niayesh K. Condition monitoring of high voltage circuit breakers: past to future. *IEEE Transactions on Power Delivery*, 2020, 36(2), 740-50.
5. Qi J., Gao X., Huang N. Mechanical fault diagnosis of a high voltage circuit breaker based on high-efficiency time-domain feature extraction with entropy features. *Entropy*, 2020, 22(4), 478.
6. Yan J., Wang Y., Wang J., et al. Zero-Shot Learning for Unknown Fault Diagnosis in High-Voltage Circuit Breakers via Envelope Spectrum Semantic Construction and Embedding[C]//2025 IEEE 8th International Electrical and Energy Conference (CIEEC). IEEE, 2025, 198-203.
7. Ye X., Yan J., Wang Y., et al. A novel circuit breaker fault diagnosis method based on dense residual and attention mechanism. *IET Generation, Transmission & Distribution*, 2023, 17(19), 4316-4328.
8. Tan Y., Hu E., Liu Y., et al. Review of digital vibration signal analysis techniques for fault diagnosis of high-voltage circuit breakers. *IEEE Transactions on Dielectrics and Electrical Insulation*, 2023, 31(1), 404-418.
9. Obarcanin K., Lacevic B. Methods for Condition Assessment of the High Voltage Circuit Breakers based on Vibration Fingerprint–A Survey. *IEEE Access*, 2025, 13, 86542-86552.
10. Geng S., Wang X. Research on data-driven method for circuit breaker condition assessment based on back propagation neural network. *Computers & Electrical Engineering*, 2020, 86,106732.
11. Asefi S., Asefi S., Afshari H., et al. Machine Learning based High Voltage Circuit Breaker Defect Classification Utilizing Savitzky-Golay Filter. *IEEE Transactions on Instrumentation and Measurement*, 2025, 74, 1-9.
12. Liu Z. Circuit Breaker Fault Detection Based on CEEMD-GSA-SVM. *Journal of Engineering*, 2025, 3.1 , 59.
13. Zheng X., Li J., Yang Q., Li C., Kuang S. Prediction method of mechanical state of high-voltage circuit breakers based on LSTM-SVM. *Electric Power Systems Research*, 2023, 218,109224.
14. Zhao S., Wang E. Fault Diagnosis of Circuit Breaker Energy Storage Mechanism Based on Current-Vibration Entropy Weight Characteristic and Grey Wolf Optimization–Support Vector Machine. *IEEE Access*. 2019, 7, 86798-809.

 doi:10.20944/preprints202601.2178.v1

15. Li X., Wu S., Li X., Yuan H., Zhao D. Particle swarm optimization-support vector machine model for machinery fault diagnoses in high-voltage circuit breakers. *Chinese Journal of Mechanical Engineering*, 2020, 33, 1-10.
16. Bie F., Zhang H., Lyu F., Lu Y., Peng J., Miao Y., et al. Research of fault information fusion based on ICEEMDAN and PSO- SVM algorithm for rolling bearing diagnosis. 2023.
17. Yang L., Zhang K., Chen Z., Liang Y. Fault diagnosis of WOA-SVM high voltage circuit breaker based on PCA Principal Component Analysis. *Energy Reports*, 2023, 9, 628-34.
18. Yang P., Li Z., Yu Y., Shi J., Sun M. Studies on fault diagnosis of dissolved oxygen sensor based on GA-SVM. *Mathematical Biosciences and Engineering*, 2021, 18(1), 386-99.
19. Xue J., Shen B. Dung beetle optimizer: a new meta-heuristic algorithm for global optimization. *The Journal of Supercomputing*, 2022, 79(7),7305-36.
20. Li X., Gu C., Chen C. Parameters Optimization of ADRC Based on DBO Algorithm. 2023 6th International Conference on Computer Network, Electronic and Automation (ICCNEA), 2023, 354-8.
21. Zhang Y., Ma T., Li T., Wang Y. Short-Term Load Forecasting Based on DBO-LSTM Model. 2023 3rd International Conference on Energy Engineering and Power Systems (EEPS), 2023, 972-7.
22. Li Y., Sun K., Yao Q., Wang L. A dual-optimization wind speed forecasting model based on deep learning and improved dung beetle optimization algorithm, *ENERGY*, 2024, 286.
23. Li L., Liu L., Shao Y., Zhang X., Chen Y., Guo C., et al. Enhancing Swarm Intelligence for Obstacle Avoidance with Multi-Strategy and Improved Dung Beetle Optimization Algorithm in Mobile Robot Navigation. Electronics, 2023,12(21).
24. Irmanda H., Astriratma R. Klasifikasi Jenis Pantun Dengan Metode Support Vector Machines (SVM). *Jurnal RESTI (Rekayasa Sistem dan Teknologi Informasi)*, 2020,4(5), 915-22.
25. Nalepa J., Kawulok M. Selecting training sets for support vector machines: a review. *Artificial Intelligence Review*. 2019, 52(2), 857-900.
26. Mohammadi M., Rashid T.A., Karim S.H.T., Aldalwie A.H.M., Tho Q.T., Bidaki M., et al. A comprehensive survey and taxonomy of the SVM-based intrusion detection systems. *Journal of Network and Computer Applications*, 2021,178, 102983.
27. Liu J., Peng X., Wu L., Li Y., Liu J., Niu S., et al., editors. Incremental learning method for online transient stability assessment of power system based on KKT condition. 2021 IEEE Sustainable Power and Energy Conference (iSPEC), 2021.
28. He Y., Chen H., Liu D., Zhang L. A framework of structural damage detection for civil structures using fast fourier transform and deep convolutional neural networks. *Applied Sciences*, 2021, 11(19), 9345.
29. Kiran . G., Parimalasundar E., Elangovan D., Sanjeevikumar P., Lannuzzo F., Holm-Nielsen J.B. Fault investigation in cascaded H-bridge multilevel inverter through fast fourier transform and artificial neural network approach. *Energies*, 2020, 13(6), 1299.
30. Alshammri, G. H. Enhancing wireless sensor network lifespan and efficiency through improved cluster head selection using improved squirrel search algorithm. *Artificial Intelligence Review*, 2025, 58, 79.
31. Shen, Z., et al. A Chaos-Initiated and Adaptive Multi-Guide Control-Based Crayfish Optimization Algorithm for Image Analysis. *Symmetry*, 2025, 17(11), 1940.
32. Mao, Z., et al. A multi-strategy enhanced dung beetle algorithm for solving real-world engineering problems. Artificial Intelligence Review, 2025, 58 (8), 253.
33. Xing, C., et al. An Improved Crested Porcupine Optimizer for Path Planning of Mobile Robot. *Applied Sciences*, 2025, 15 (23), 12595.
34. Christiyana, C. C., et al. Enhancing breast cancer detection: a novel residual radial kernel support vector-based stain bower search algorithm. *International Journal of Machine Learning and Cybernetics*, 2025, 16 (12), 10851-10869.
35. Yan, J., et al. Few-shot mechanical fault diagnosis for a high-voltage circuit breaker via a transformer–convolutional neural network and metric meta-learning. *IEEE Transactions on Instrumentation and Measurement*, 2023, 72, 1-11.

 doi:10.20944/preprints202601.2178.v1